SURFACE-INITIATED ATOM TRANSFER RADICAL POLYMERIZATION OF MAGNETO-OPTICALLY ACTIVE NANOCOMPOSITES: ROLE OF RANDOM COPOLYMERS FOR HIGH VERDET CONSTANT MATERIALS

By

JESSICA ALEXANDRA VICKERY

_____

A Thesis Submitted to The Honors College

In Partial Fulfillment of the Bachelors degree
With Honors in

Biochemistry

THE UNIVERSITY OF ARIZONA

M A Y 2 0 2 1

Approved by:

_____

Prof. Jeffrey Pyun
Department of Chemistry and Biochemistry

Acknowledgments

I would like to thank Professor Jeffrey Pyun for the support and mentorship during my undergraduate education. Professor Pyun has guided me in my research and allowed me to develop my organic chemistry laboratory skills for the past two years. I would also like to thank Lindsey Holmen for training and supporting me in my thesis research endeavors. Lindsey, as a graduate student, has played a large role in the direction and understanding of this research project. Lastly, I would like to thank the rest of the members of the Pyun Group and Norwood group who have helped me obtain data and develop my laboratory skills.

The Chemistry and Biochemistry department advisors have also played an important role in my undergraduate education. I would like to thank Olivia Mendoza and Christine Gronowski for guiding me throughout my undergraduate years.

Abstract

Magneto-optically active materials play a crucial role in detection of weak magnetic fields produced by biological systems and are a key component in optical communications systems. Michael Faraday discovered that applications of magnetic field to a lead-doped piece of glass induced rotation of linear polarized light propagating through the glass in 1845. This is now known as the Faraday effect and the strength of this effect is described by the Verdet constant; a wavelength and compositionally dependent quantity. Currently, inorganic crystals containing paramagnetic ions are used to rotate light in traditional systems; however, processing limitations and low Verdet constants require new materials to be explored. In previous work, a new approach in fabrication of high-Verdet material was done by utilizing a matrix of polymer coated cobalt ferrite nanoparticles ($CoFe_2O_4$) and high molecular weight polystyrene to fabricate magneto-optically active films.[1] In this work, we have a similar end goal however the matrix is made up using surface-initiated atom transfer radical polymerization (SI-ATRP) with cobalt nanoparticles (CoNPs) and a varying amount of two monomers to effectively attempt to improve physical properties. This was done by comparing SI-ATRP with pure methyl methacrylate (MMA) to copolymers that contain small amounts of n-butyl-acrylate (nBA) to introduce rubbery components to a glassy matrix. Three SI-ATRP reactions were performed, one with pure MMA and two copolymerizations with MMA and nBA that had a target composition of 90:10 and 70:30 (MMA: nBA). From this research, we found that as the polymer had a higher molar ratio of nBA, the melt pressed thin films became more brittle and less transparent. This effected our measurement of Verdet, specifically in the 70:30 sample, which could not be measured. However, we found that the 90:10 (MMA-*r*-nBA) sample had a Verdet constant of 119,800 °/Tm comparative to the control sample of pure MMA, which had a Verdet constant of 84,360 °/Tm. Further polymer and composite characterization was analyzed using size exclusion chromatography (SEC), nuclear magnetic resonance (NMR), thermogravimetric analysis (TGA), and differential scanning calorimetry (DSC).

Introduction

Magneto-optically active materials are found in photonic devices, as optical isolators, circulators, switches, magneto-optic modulators, and high-performance magnetic field sensors.[13] Particularly, optical isolators find extensive use in commercial high-powered laser and communications systems, preventing unwanted feedback of reflected light into the source resonant cavity. In 1845, Michael Faraday discovered the Faraday effect, one of the fundamental magneto-optic (MO) effects which describes the influence of an applied magnetic field on polarized light passing through a MO active material.[15] When a magnetic field parallel to the direction of light propagation is applied, a rotation of the polarization plane of linearly polarized light is observed from a field induced circular birefringence along the axis of the applied field. This effect for a material is quantified by the material's Verdet constant (V), which is a wavelength and temperature dependent constant; the resulting polarization rotation (θ) is the product of V, the applied magnetic field (B) and the path length (L) of light through the material (Figure 1).

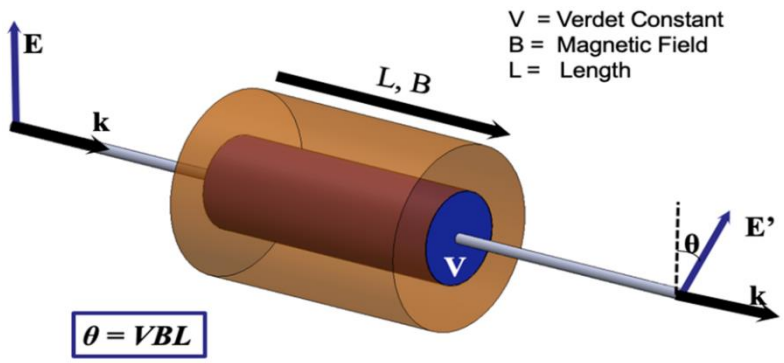

Figure 1. *Faraday Effect. Rotation of the plane of polarization of a light beam by a magnetic field. The magnetic properties of cobalt nanoparticles create this phenomena and sensitivity to light can be characterized by the Verdet constant.*

This relationship is shown by equation (1).

$$\theta = VBL \qquad (1)$$

Specifically, for optical isolation and magnetic sensing large path lengths and high Verdet constants are needed to enable orthogonal polarization of reflected beams and sensitive magnetic field detection. For these applications, the most common material in the visible to near infrared (NIR) spectrum is terbium gallium garnet (TGG, V_{TGG}=2.2X 10^3 °/Tm at 1310nm). These ferromagnetic, rare-earth based crystals are highly stable and transparent; however, these materials are limited by lower Verdet constants and substantial temperature dependence. Furthermore, these materials are usually prepared as single crystals, which introduces challenges to device fabrication and integrated photonic applications due to crystallinity of the rotators. However, a challenge that remains for the fabrication of low-cost alternatives to traditional garnet crystals is the creation of processable materials with both high Verdet constants and high transparency, especially in the NIR. For this reason, many

efforts have been made to develop polymer-based analogues to the ferromagnetic garnets, with semi-conducting polymers and nanoparticle-polymer composite systems. Recent work by Swager *et al.* demonstrates high Verdet constants of up to 7.6×10^4 °/Tm for sulfone-containing chiral helical polythiophenes at 532nm.[6] Prasad and co-workers also reported on tuning magneto-optic (MO) activity by doping organic biradicals into polyfluorene chiral helical polymers and obtaining Verdet values of up to 380,000 °/Tm at 410nm.[7] These two studies emphasize the strong effects of nanoscopic ordering and architecture on MO activity and provide principles for the design of polymer systems with high Verdet constants. However, the wavelength dependence of the MO activity of these systems often requires measurements at values proximal to absorption bands. Furthermore, for these all-organic systems high fields for measurement (0.5-1.5T) are required due to difficulty in scaling and processing of these materials to support thick films with large rotations, limiting their application.

An alternative, low-cost approach towards materials with improved Faraday rotation involves the incorporation of high Verdet nanoparticles (NPs) into polymer matrices to generate MO active nanocomposites. Due to the tunable properties of the MO active nanoparticles, these materials have the advantage of potentially high Verdet constant values off-resonance from primary absorption bands. The classical magnetic properties of a single isolated nanoparticle are well known; however, particle effects on MO properties of a material are a new area of research. The incorporation of magnetic nanoparticles into sol-gel or polymer matrices has been explored for this application. While, wholly inorganic composites are superior in terms of matrix stability, porosity induced scattering of light has been shown to limit the performance of sol-gel and inverse opal-based systems. Aggregation of nanoparticles in polymer-nanoparticle composites at appreciable loadings (>1wt% loading) severely limit the Faraday effect in these materials. Despite these challenges, previous work to improve nanoparticle dispersion in polymer matrices by surface functionalization of magnetic nanoparticles enabled fabrication of relatively thick films with high Verdet constant values in the NIR. Previous work by Peyghambarian and coworkers has demonstrated Verdet constants of up to 8.0×10^4 °/Tm at 1310nm for polymethylmethacrylate (PMMA) grafted Fe_3O_4 nanoparticles crosslinked in a PMMA matrix.[8-11] However, loss of MO activity had been observed over time for Fe_3O_4 based materials. In recent work, Watkins and coworkers reported the preparation of MO active nanocomposites with enhanced Faraday rotation and dispersion qualities by the introduction of gallic acid functionalized FePt nanoparticles into polystyrene-*block*-poly-2-vinylpyridine templates, allowing for high nanoparticle loadings of up to 10 wt% into the final multilayer films. By variation of nanoparticle size

and loading, Faraday rotations could be tuned from 0.98-2.79x10^4°/Tm at 1310nm for these thin films.[12]

With potential for high Verdet composites prepared from magnetic nanoparticles, there is a need for versatile methods to functionalize magnetic NPs with ligands to promote dispersion into polymeric material. In previous work, we have demonstrated that end-functional polymeric ligands prepared by atom transfer radical polymerization (ATRP) are capable of promoting the growth of well-defined ferromagnetic cobalt NPs and functionalization reactions via ligand exchange onto CoNPs. However, the use of the end-functional polymeric ligands has not been applied to functionalization and dispersion of magnetic NPs for use in MO applications. This approach may allow for modular variation of both NP and polymeric components. Furthermore, we have fabricated MO active polymer-nanoparticle composite films with a Verdet constant up to ten-fold greater than commercially available TGG crystals in the NIR region. These devices were prepared with 5nm $CoFe_2O_4$ NPs functionalized with carboxylic acid terminated polystyrene ligands (PS-COOH) which enabled their dispersion in high molecular weight polystyrene matrices.[1] The fabrication of alternating layered polymer films was prepared by sequential spin coating of high Verdet constant NPs loaded polystyrene films.

For this research work, surface-initiated atom transfer radical polymerization (SI-ATRP) was utilized for synthesis of a polymer-nanoparticle composite. Originally, methyl methacrylate (MMA) was used as the only monomer in the reaction and provided a glassy matrix for thin films. Copolymerization was the focus of this study where n-butyl-acrylate (nBA) was polymerized along with MMA during synthesis of polymer-nanoparticle composite via SI-ATRP. nBA was chosen as the second monomer in the polymerization because it has rubbery properties and would lower the glass transition point (Tg) relative to PMMA (poly(methyl methacrylate)), since PBA (poly(n-butyl-acrylate)) and PMMA have a Tg of -45°C and 100°C, respectively.[16] The goal was to make a polymer nanoparticle composite with both rubbery (nBA) and glassy (MMA) components with anticipation that the growth of rubber copolymers of poly(BA-*r*-MMA) would impart enhanced ductility to hybrid nanoparticles that otherwise afford highly brittle materials with poor film forming properties. Furthermore, various ratios of MMA to nBA were used in two separate reactions with the attempt of synthesizing a copolymer nanoparticle material with 90:10 and 70:30 molar ratio (MMA: nBA). The purpose of making a rubbery copolymer material is to fabricate a more pliable and higher Verdet constant material with the goal of preventing nanoparticle aggregation in thin films. Polystyrene coated cobalt nanoparticles (CoNPs) were chosen for this material synthesis utilizing one-pot ligand

exchange with phosphonic acid and CoNP ferrofluid. Each material sample was analyzed for polymer and nanocomposite characterization and compared to a control material that was synthesized with only MMA, as a homopolymer. All three materials were melt-pressed for thin film fabrication and further Verdet constant and transmission measurements.

Methods and Materials

Total Synthesis

The total synthesis strategy used to prepare these new copolymer-magnetic NP materials was the following: (1) synthesis of polymer coated cobalt NPs (2) synthesis of new halo-functional phosphonic acid ligands (3) in situ ligand exchange and surface initiated ATRP.

Preparation of Precursors for Surface Initiated ATRP from Magnetic Particles

First, synthesis of low molecular weight carboxylic acid terminated polystyrene (PS-COOH) was performed via ATRP. All of these materials were prepared using the prior reported methods of Pyun *et al.* [4-5] PS-COOH was produced to enable diverse functionalization of magnetic NPs and further promote dispersion in polymeric films. PS-COOH was then directly used in the synthesis of cobalt nanoparticles (CoNPs) as the surface ligand, to prevent aggregation of these very highly magnetic particles. A 250 mL three necked round bottomed flask (TNRBF) was flame dried under vacuum and set up to a reflux condenser. Next, a 100 mL round bottomed flask (RBF) was flame dried under vacuum with a stir bar and 40 mL of dry 1,2-DCB was added to the flask and purged with argon. Then, 0.8 g of PS-COOH and 2.5 g of $Co_2(CO)$ were added to the flask and stirred at 1200 rpm. The flask was purged with argon for 30 minutes and then heated to 170°C. The reaction was allowed to continue for 4 hours (Figure 3).

A multi-step synthesis of a phosphonic acid surface ligand was performed in order to replace PS-COOH with a small molecule ATRP initiator, effectively functionalizing the surface of the CoNPs (Figure 2). The first step of this synthesis includes DHP protection of 11-bromo-1-undecanol. In a 250 mL RBF, (10g, 39.8mmol) of 11-bromo-1-undecanol was dissolved in 50 mL of THF. 10mL, 109.6mmol of 3,4-duhydro-2H-pyran was added dropwise and, after stirring for five minutes, (0.070g,

0.37 mmol) p-TsOH was added. The reaction was left stirring over night at room temperature.

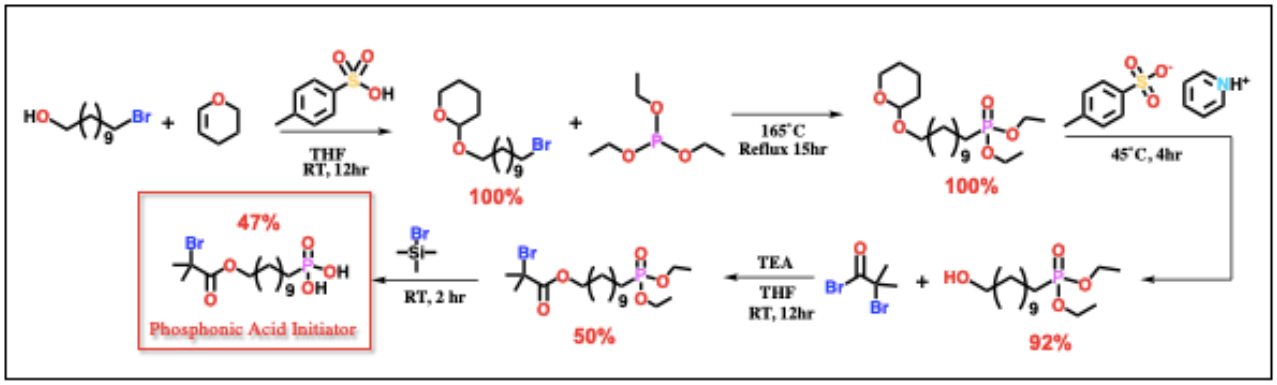

***Figure 2**. Phosphonic Acid Multi-Step Synthesis. Step one and two had a 100% yield. Step three had a 92% yield. Step four had a 50% yield and step five had a 47% yield. The product was utilized in one-pot ligand exchange.*

After the reaction was left overnight, the organic phase was washed two times with 60 mL of Na_2CO_3 and one time with 60 mL of water. The organic phase was dried over $MgSO_4$ and separated using gravity filtration. The solvent was then evaporated off using rotary evaporation. This would yield a yellowish liquid of 11-bromo-1-(tetrahydropyranyloxy)undecane. The second step includes the phosphonation of 11-bromo-1-(tetrahydropyranyloxy)undecane. This step of the synthesis was performed by adding (16.53 mL, 96.4 mmol) triethyl phosphite to 11-bromo-1-(tetrahydropyranyloxy) undecane and left to react at 165°C under reflux for 15 hours. Excess triethyl phosphite was evaporated and the product was a yellow liquid. The third step is the deprotection of 11-(Diethyl phosphonyl)-1-(2-tetrahydropyranyloxy) undecane. To perform this step the product from the second step was placed in a reaction flask with (0.1073g,0.427 mmol) pyridinium p-toluenesulfonate and 30 mL of methanol. The reaction was left to react for four hours at 45°C while stirring. After four hours, the reaction was set to cool to room temperature and then 50 mL of DCM (dichloromethane) was added. Next, the organic layer was washed three times with saturated NaCl solution and dried over $MgSO_4$, filtered using gravity filtration, and solvent was evaporated.

The fourth step consists of esterification of 11- (diethyl phosphonyl) undecanol. This step was performed by adding (12.16g, 39.42 mmol) 11- (diethyl phosphonyl) undecanol with (10.99 mL, 78.84 mmol) triethylamine (TEA) and 40 mL of anhydrous THF. 9.75 mL, 78.84 mmol of α-bromoisobutyryl bromide was dissolved in 20 mL of THF and was added dropwise to the reaction flask. The reaction was stirred over night at room temperature under reflux and then diluted with 30 mL of hexanes. The organic layer was washed with 1M aqueous HCl twice and then three times with water. This organic phase was dried over $MgSO_4$ and filtered. THF was evaporated and the light-

yellow liquid was purified by column chromatography with ethyl acetate as the eluent. This step provides a light-yellow oil as the product. Lastly, the formation of 11-(2-bromoisobutyrate)-undecyl-1-phosphonic acid using bromotrimethylsilane was established. The final step of this synthesis was performed by adding (8.84g, 19.33 mmol) 11-(2-bromo-2-methyl)-propionyloxy)-undecyl-1-diethylphosphonate ester to a reaction flask with a septum and reflux condenser. Bromotrimethylsilane (7.65 mL, 57.99 mmol) was then added dropwise to the flask. The mixture was stirred at room temperature for 2 hours and then 30 mL of methanol was added to the reaction. This was left to stir for another 4 hours. The product was recrystallized in a hexanes/DCM mixture, producing a pure white powder of 11-(2-bromoisobutyrate)-undecyl-1-phosphonic acid. The use of 1H and 13C NMR spectroscopy of isolated compounds in this synthesis were used to confirm target molecule structure and purity. Mass spectrometry was deemed unnecessary since these compounds have been previously reported.[17-18]

One-pot Ligand Exchange via Ultrasonication

The unpurified ferrofluid containing polystyrene coated CoNPs from the CoNP synthesis is split up into smaller volumes and used for ligand exchange. An appropriate amount of phosphonic acid initiator (based on PS-COOH content) is directly added to the small volume of ferrofluid and probe sonicated for five hours in order to promote the ligand exchange (Figure 3). In most cases, ligand exchange of inorganic nanoparticles is conducted by isolation of re-dispersed colloids in solution with externally added ligands. This is done with the addition of heat or other energy inputs to drive the exchange and attachment of ligands to NP surfaces. In this case with magnetic cobalt nanoparticles, isolation of PS-CoNPs may result in undesirable NP aggregation due to the magnetic associative nature of these metals. Hence, we employed, for the first time, a one-pot method where the original dispersed reaction mixture of PS-CoNPs were treated with phosphonic acid ligands and then subjected to sonication of the reaction medium using a high-power sonication horn. Under these conditions, the high shear forces generated by the sonication process enable both ligand exchange of PS-COOH ligands with phosphonic acids and further drives covalent condensation of phosphonic acids to the

magnetic NP surface. This new process greatly expedites the ligand exchange reaction while also preserving NP dispersion.

SI-ATRP with Ferromagnetic Cobalt Nanoparticles

Surface-initiated atom transfer radical polymerization was conducted to form a growing polymeric shell around the CoNPs with controllable molecular weights. The first SI-ATRP was performed with pure methyl methacrylate (MMA), which served as the control, and two additional SI-ATRP reactions were performed to compare the physical properties of the films when varying amounts of n-butyl acrylate (nBA) are added. All SI-ATRP reactions were performed using standard ATRP techniques with a target degree of polymerization (DP) of 300.[14] The general procedure involves adding CuCl (0.0334 g, 0.337 mmol) and dNbpy (0.2068g, 0.506 mmol) to a Schlenk flask and executing air-free techniques to assure no oxygen is present. Pure uninhibited and purged MMA (5.076mL, 50.7 mmol) was added to the Schlenk flask and left to stir to allow for the catalyst and ligand to complex together. Lastly, 3mL of purged ferrofluid from the one-pot ligand exchange containing CoNPs and dichlorobenzene (DCB) was added into the reaction flask. The reaction was then heated to 75°C and allowed to react for 20 hours. For the copolymerization of MMA and nBA with CoNPs the same protocol was followed in the same order of steps; however, using 90:10 and 70:30 (MMA: nBA) compositions. We anticipated that the higher PBA content in the polymer would lower Tg of hybrid copolymer NPs, which would enhance the film forming properties of these materials. Once polymerized, all samples were dissolved in tetrahydrofuran (THF) and precipitated into hexanes to yield a grey powder.

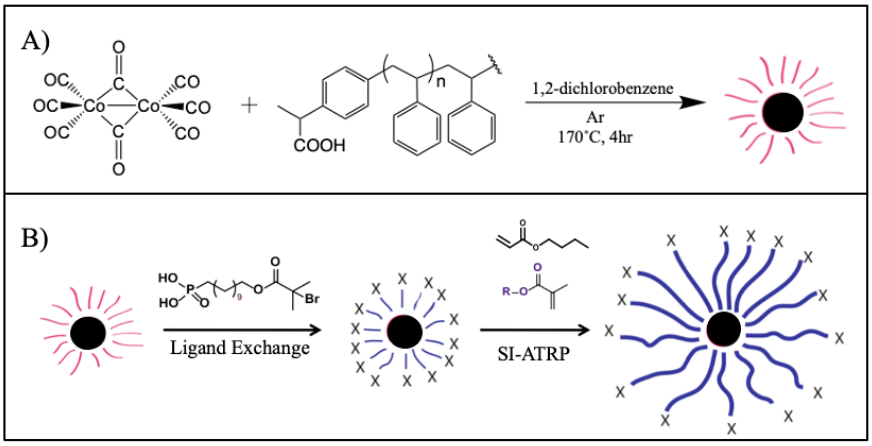

Figure 3*. CoNP Synthesis and SI-ATRP.* ***A.*** *Dicobalt octacarbonyl was reacted with carboxylic acid terminated polystyrene in 1,2-dichlorobenzene at 170°C for 4 hours to synthesize polystyrene coated cobalt nanoparticles.* ***B.*** *One- pot ligand exchange via ultrasonication with ferrofluid of CoNPs and phosphonic acid was performed. Polystyrene was replaced with phosphonic acid to functionalize the surface of the CoNPs. Lastly, SI-ATRP with n-butyl acrylate and methyl methacrylate was conducted to grow polymer onto surface of the CoNPs.*

Thin Film Fabrication by Melt-Pressing

To fabricate thin films from each polymer nanoparticle material using the method of melt pressing a small amount of material was placed on a glass slide and heated to 200°C by a hot plate. It was then pressed down between another glass slide. The material was removed from the glass slide and placed in a 2-ton manual hydraulic press. The thin films were created by pressing this material with 0.75 tons of pressure and heating it to 200°C. Each thin film was made to have a thickness of 111μm.

Evaluation of Polymer Characterization

At the end of each SI-ATRP that was performed, a small amount (0.1mL) of the polymer-nanoparticle composite dissolved in THF was taken for polymer characterization and dissolved in 2mL deuterated chloroform. In each of these samples, cobalt nanoparticles were digested by concentrated hydrochloric acid (HCl) and were passed through an alumina plug. This preparation of the samples allowed for the use of nuclear magnetic resonance (NMR) for calculation of percent conversion of each monomer into polymer. NMR functions as a way to characterize the polymer's structure from the various resonance frequencies of protons within the polymer. Nuclei in a strong constant magnetic field are perturbed by a weak oscillating magnetic field and respond by producing an electromagnetic signal with a frequency characteristic of the magnetic field at the nucleus. Monomer conversion in the SI-ATRP process was calculated by comparing between monomer and polymer integration peaks in the NMR.

Molecular weight and polydispersity of each polymer synthesized was determined using size exclusion chromatography (SEC). The same samples that were used previously for NMR were also used for the SEC. The deuterated chloroform was evaporated from these samples and the samples were dissolved in 0.7mL of anhydrous THF. These samples were then filtered through syringe filters and injected for gel permeation chromatography (GPC) to obtain a relative molecular weight of the grafted polymer.

Evaluation of Nanocomposite Characterization

Transmission Electron Microscopy (TEM) was utilized for the visualization of cobalt nanoparticle dispersion among the polymer matrix of each polymer-magnetic NP composite made. Each sample was added dropwise to a carbon coated copper grid that would allow for imaging via TEM. Once each sample dissolved with THF as a solvent was dropped on a grid, the grid was allowed to dry for the solvent to evaporate. These grids were placed in the transmission electron microscope

and viewed to determine interparticle spacing, sizing of CoNPs, and if polymerization successfully separated the cobalt nanoparticles.

Thermogravimetric analysis (TGA) is a method of thermal analysis in which the mass of a sample is continuously measured over time as temperature is increased. This analysis provides us with information on the percentage of organic and inorganic content, as well as thermal decomposition of the material. TGA was performed on all three samples of precipitated polymer-magnetic NP material. Furthermore, differential scanning calorimetry (DSC), a thermoanalytical technique in which the heat flow (in and out) of a sample is measured as a function of temperature, while the sample is exposed to a controlled temperature program was utilized to gain more information on the thermal properties of these samples. From this analysis, we can find crystallinity, glass transition temperature (Tg), and melting temperature as the polymer-magnetic NP composite transitions throughout differing temperatures.

Magneto-Optic Activity Characterization of Thin Films

In order to measure the Verdet constant of these thin films, a percent transmittance of 15% or greater, at 1310 nm, needs to be achieved. Once this is confirmed through UV-Vis spectroscopy,

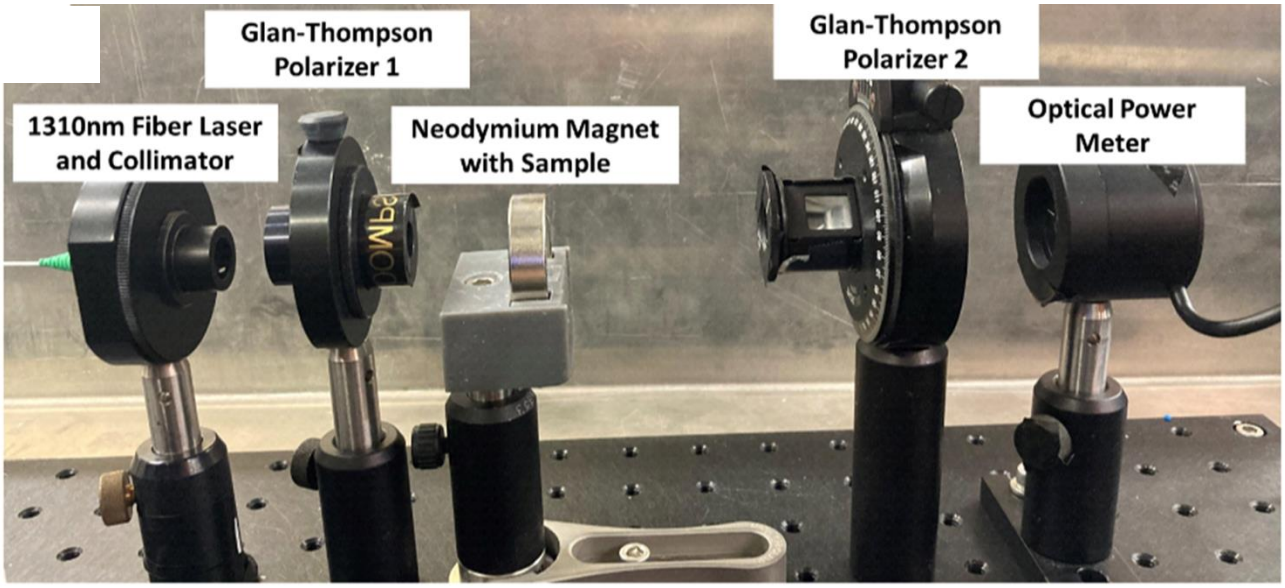

Figure 4*. Measurement set up to determine the total Faraday rotation of light passing through the material, (measurement of Verdet constant for melt pressed thin films).*

the MO activities of the polymer-magnetic NP composite thin films were evaluated via the experiment set up shown in Figure 4, under an applied magnetic field. The Verdet constants were measured in a custom-built system consisting of a 1310nm Fabry-Perot laser where the output polarization is controlled using a half wave plate in conjunction with a high extinction ratio Glan-Thompson

polarizer. This light passes through a non-polarizing beam splitter (NPBS), and then interacts with the sample placed in the solenoid. The gold backing of the multi-film stack then reflects the light through the sample again and back to the NPBS. The light that is reflected by the NPBS then passes through a Wollaston prism that separates this light into the *s* and *p* polarized components. A lens is then used to focus these beams onto the detector components of a 2017 Nirvana auto-balanced optical receiver. The input polarization of the laser source is set to be at 45° after leaving the polarizer, so the irradiance on both sides of the detector is of nominally equal magnitude.

A sinusoidal current at 100Hz is generated by a Stanford Research Systems SR830 lock-in amplifier. This current is amplified by a Bose PowerShare PS602 amplifier which then drives the solenoid holding the sample. The Nirvana is connected to the lock-in amplifier, such that the Stanford lock-in can pick up the AC fluctuation between the difference of the *s* and *p* polarized light beams resulting from the change in magnetic field. As measurements are taken, the current used to drive the solenoid is increased, and the AC fluctuation signal at 100Hz and the DC signal on the differential detector were recorded by a computer program. A Lakeshore 421 gaussmeter was used to measure the magnetic field at the sample for these various driving currents to the solenoid. Verdet measurements were obtained from this experimental design to gain information on the MO activities of these samples.

Results

SI-ATRP Copolymer Characterization

To analyze the composition of copolymer that was made, nuclear magnetic resonance (NMR) and size exclusion chromatography (SEC) were performed on all samples. From the NMR we were able to calculate the percent conversion of each monomer into the overall polymer of each sample using the integration peaks from monomer and polymer. We found that the control sample of pure poly(methyl methacrylate) (PMMA) reached full conversion (100%) of MMA monomer into PMMA. The sample that had a targeted molar ratio of 90:10 (MMA: nBA) had a 77.3% MMA conversion to PMMA and a 61.4% conversion of nBA into PBA (poly(n-butyl-acrylate)) and appeared very viscous in the reaction flask at the end of synthesis. Furthermore, the sample that had a targeted molar ratio of 70:30 (MMA: nBA) had a 30.8% conversion of MMA to PMMA and an 18.3% conversion of nBA into PBA and was seen as being drastically less viscous than the other two samples at the end of the reaction.

In relation to these results, the percent conversion was utilized for the calculation of the actual molar ratio of each polymerization. From these calculations, it was found that the 90:10 targeted molar ratio copolymerization had an actual molar ratio of 91.89: 8.11 (MMA: nBA), while the 70:30 molar ratio had an actual ratio of 79.7: 20.3 (MMA: nBA). Molecular weights and polydispersity of the polymers were evaluated by SEC (Figure 5). Isolated PMMA was cleaved from CoNPs in the control sample for characterization by SEC (Mn=128,049g/mol; Mw/Mn=1.064). Furthermore, isolated 90:10 molar ratio copolymer was cleaved from CoNPs for characterization by SEC (Mn=125,511g/mol, Mw/Mn=1.105). Lastly, isolated 70:30 molar ratio copolymer was evaluated by SEC (Mn=68,956g/mol, Mw/Mn=1.076). In the SEC data, a peak for polystyrene is seen for all samples because of its presence in the solution after the one-pot ligand exchange with phosphonic acid. The separation of polystyrene from the sample has been a continuing challenge for this synthesis.

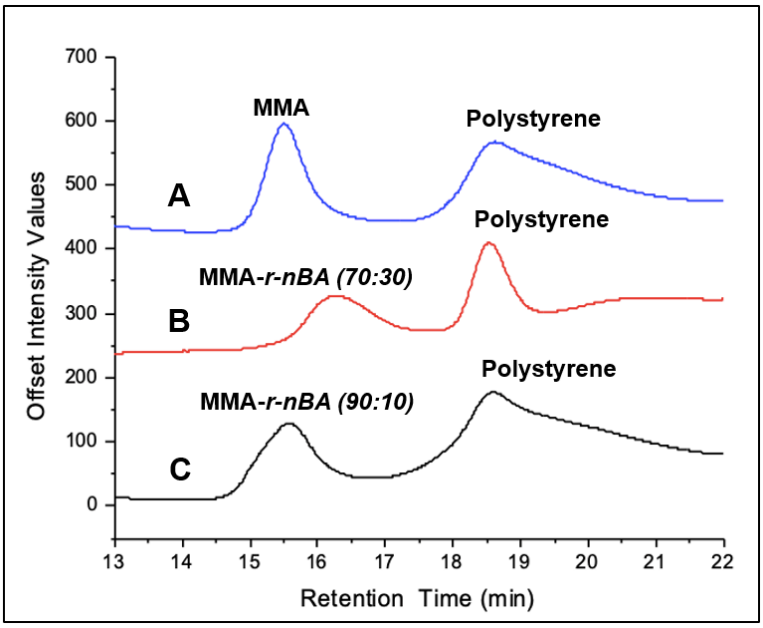

***Figure 5**. Size Exclusion Chromatography graph. **A**. Control PMMA, (Mn=128,049g/mol; Mw/Mn=1.064) **B**. Copolymer with molar ratio of 70:30 (MMA: nBA), (Mn=68,956g/mol, Mw/Mn=1.076). **C**. Copolymer with molar ratio of 90:10 (MMA: nBA), (Mn=125,511g/mol, Mw/Mn=1.105). Polystyrene was found in all size exclusion chromatography due to the difficulty of separating it from the material.*

Finding that the pure PMMA sample had full conversion, while the copolymers had lower conversion illustrates the competitive polymerization between these two monomers. Furthermore, the rate of MMA polymerization is greater than nBA. This can be explained by the more reactive properties of the tertiary radical on MMA compared to the less reactive secondary radical on nBA. For this reason, the 70:30 molar ratio sample had lower conversions and molecular weight due to the higher ratio of PBA in the polymer and higher probability of polymerization competition between monomers. This reasoning may also be true for the 90:10 molar ratio sample explaining its slightly lower percent conversion values and molecular weight compared to the PMMA control sample.

Polymer-Nanoparticle Composite Characterization

Thermogravimetric analysis (TGA) data provided the temperature at which decomposition begins and the weight percent of organic and inorganic material in these samples. The temperature at which decomposition began for the control PMMA sample was 200°C, the 90:10 sample had decomposition begin at 225°C, and the 70:30 sample had decomposition begin at 225°C, as well. The percent weight loading for the control PMMA sample was 2.34-wt% of CoNPs, meaning that 97.66-wt% was made up of PMMA. The 90:10 sample had a percent weight loading of 2.51-wt% of CoNPs and the rest of the weight was made up of copolymer. Lastly, the 70:30 sample had a 6.85-wt% of CoNPs. This sample had a higher weight percent of nondegradable nanoparticles compared to the control and the 90:10 sample due to its lower percent conversion of polymer, which led to more space in the material for cobalt nanoparticles due to less polymer in the material.

Differential scanning calorimetry (DSC) measurements were done to find the thermal softening point or glass transition temperature (Tg) for each polymer-nanoparticle composite. PMMA has a Tg of 100°C and PBA has a Tg of -45°C. Copolymerization of these two creates a material with a mixture of these two thermal properties and the Tg of these materials synthesized was measured with DSC. It was found that the control with PMMA had a Tg of 100°C. Comparatively, the 90:10 sample was measured to have a Tg of 85°C and the 70:30 sample was measured to have a Tg of 75°C. Both of the copolymer samples had a lower Tg compared to the control due to the lower standard Tg of PBA and in copolymerization of these two monomers the thermal softening point decreases. Furthermore, only one lower Tg was found on the DSC for the MMA-*r*-nBA material and this provides evidence that there is a new polymer shell from SI-ATRP because the Tg of PMMA at 100°C in these samples is not found.

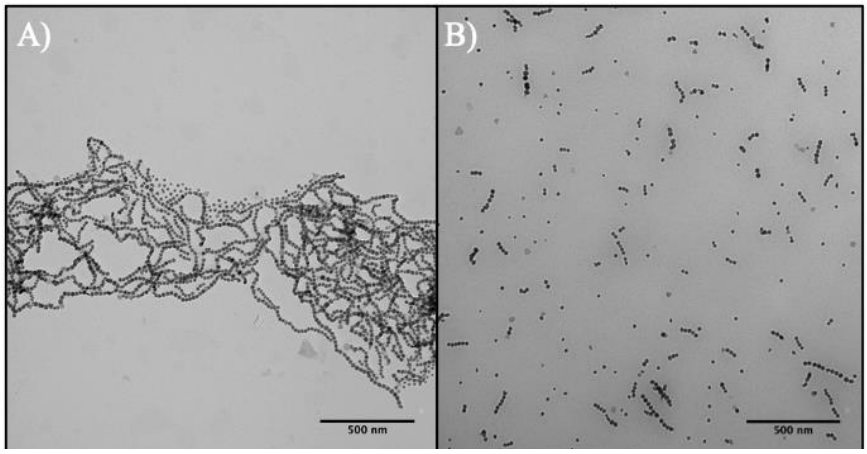

***Figure 6**. Transmission electron microscopy (TEM) images **A.** Polystyrene coated cobalt nanoparticles chaining prior to SI-ATRP. **B.** Cobalt nanoparticle separation after one pot ligand exchange with phosphonic and polymerization via SI-ATRP.*

Transmission electron microscopy (TEM) images show the dispersion of nanoparticles among polymer. Polymerization aids in preventing aggregation of the nanoparticles as seen in the image of the chained nanoparticles before SI-ATRP and after (Figure 6). Furthermore,

the TEM image after polymerization displays a difference in the way nanoparticles are aggregated and provides evidence that polymerization created spacing between CoNPs.

Melt-Pressed Thin Film Evaluation

The resulting grey solid that was obtained from each SI-ATRP reaction was fabricated into free standing melt-pressed thin films. Upon completion of melt-pressing it was observed that the thin films with MMA-*r*-nBA were more brittle and difficult to press compared to the control (Figure 7). This challenge was greater as the amount of nBA polymerized in the material was greater, specifically in the 70:30 thin film. Furthermore, each thin film was placed up against a source of light to qualitatively visualize the transparency of the films. It was found that the PMMA and MMA-*r*-nBA (90:10) thin film had similar transparency where visible light was able to pass through the film. However, the 70:30 (MMA-*r*-nBA) sample had minimal light that was able to pass through the film, giving it low transparency, comparatively.

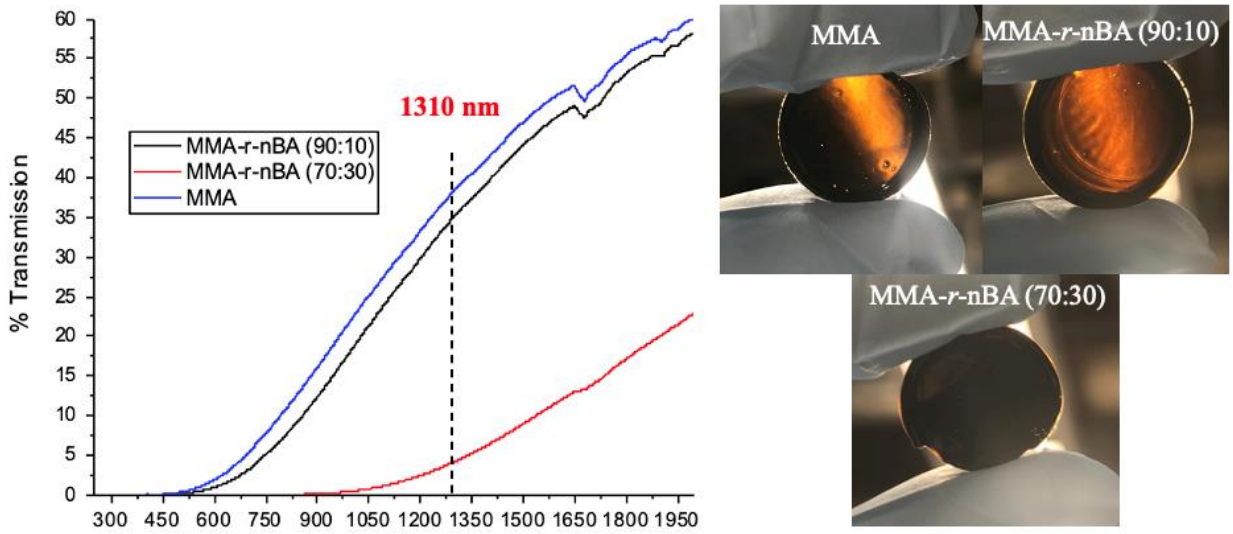

Figure 7. *Optical Transmission of Melt Pressed Thin Films. % transmission for each thin film at a wavelength of 1310nm (left). MMA (38% transmission), MMA-r-nBA (90:10) (34% transmission), and MMA-r-nBA (70:30) (4% transmission). Images of melt pressed thin films placed in front of a visible light source (right). MMA (control) and MMA-r-nBA (90:10) thin films are similarly transparent, while the MMA-r-nBA (70:30) thin film had minimal transparency. All thin films had a thickness of 111μm.*

To measure the magneto-optic activity by Verdet measurement for these thin films, transparency of the material is needed. Optical transmission at 1310nm is crucial for the ability to measure Verdet in these samples. For this reason, each of these thin films underwent optical transmission testing. From these tests, it was found that at the wavelength of 1310nm, the PMMA control film had a 38% transmission, the MMA-*r*-nBA (90:10) film had a 34% transmission, and the MMA-*r*-nBA (70:30) film had a transmission of 4%. To be able to measure Verdet the optical

transmission at 1310nm must be at least 15%. Due to these limitations, the MMA-*r*-nBA (70:30) thin film was unable to undergo Verdet analysis; however, the control and 90:10 thin films were able to be evaluated.

The very low transmission of the MMA-*r*-nBA (70:30) thin film can be explained by the low conversion from monomer to polymer in this material. Due to low conversion and slower rate of polymerization, formation of effective copolymer to separate the CoNPs in the material was not achieved. In this case, the CoNPs had more space to fill in the material due to less copolymer being present. The polymerization plays an important role on the transparency of the material and when polymer is low in the material, the transparency decreases and light is unable to pass through the thin film.

Magneto-Optic Activity Characterization of Thin Films

The Verdet constant of the PMMA (control) thin film was measured to be 84,360 °/Tm and for the MMA-*r*-nBA (90:10) thin film it was 119,800 °/Tm (Figure 8). The MMA-*r*-nBA (90:10) thin film had almost 1.5 times higher Verdet than the control, which provides evidence that copolymerization at smaller molar ratios of nBA is successful in this system and this material has a generally high Verdet magneto-optic activity compared to a commercially available TGG crystal and the control material that has been originally used for this system. However, the MMA-*r*-nBA (90:10) thin film had a lower transmission at 1310nm compared to TGG, which has an 80 percent transmission at this wavelength. The fabrication of material that has both a high Verdet constant and high percent transmission at 1310nm has been a continual challenge when making magneto-optically active materials that can be used commercially in photonic devices.

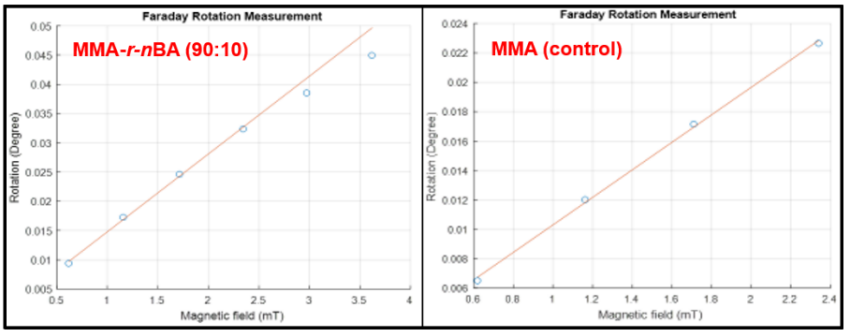

Composite	Verdet Constant (°/Tm)	% Transmission
MMA	84,360	38 %
MMA-*r*- nBA (90:10)	119,800	34 %
MMA-*r*- nBA (70:30)	-	4 %

Figure 8*. Measurement of Verdet Constants. MMA-r-nBA (70:30) thin film was not measured due to low percent transmission at 1310nm.*

Discussion

In light of the results found by this work, copolymerization via SI-ATRP was successful in obtaining a high Verdet magneto-optically active material, specifically in the MMA-*r*-nBA (90:10) material. Introducing rubbery monomer (nBA) into SI-ATRP with the glassy monomer of MMA that was previously used for this system has increased the Verdet constant of the material, comparatively. In this work, we have demonstrated the effectiveness of melt processing for fabricating thin films rather than a solution processing method used in previous work. By testing two different molar ratios of each monomer, MMA and nBA, for polymerization, a better understanding of mechanical and thermal property optimization has been achieved. We have found that at higher molar ratios of nBA added to the polymerization, the glass transition temperature decreases, lower percent conversion in polymerization is obtained, and thin films become more brittle and less transparent. This can be attributed to the competition of both monomers to polymerize in SI-ATRP, which creates a smaller surface area of polymer, more aggregation of CoNPs, and overall lower transmission of light for thin films.

However, a low molar ratio, such as one below 10%, for nBA may provide the redeeming properties of this rubbery monomer to polymer-nanoparticle composites without the downfalls found here in copolymerization. Furthermore, we have a defined a way to determine conversion and molecular weight of these materials; however completely purifying the SI-ATRP material from free polymer is still a challenge. In future research, the separation of free polymer can be explored to further purify the material. Now that copolymerization for this system has been proven to be successful, new copolymerizations with different monomers at varied molar ratios can be investigated, as well. Lastly, research on various thicknesses of thin films and their effects on Verdet and light scattering can be done to gain knowledge on how to improve transmission at 1310nm.

Conclusion

In summary, we report for the first time the copolymerization of methyl methacrylate and n-butyl-acrylate with cobalt nanoparticles utilizing surface-initiated atom transfer radical polymerization, one-pot ligand exchange, and melt-press fabrication of thin films. This is the first demonstration of using the SI-ATRP process to grow rubber copolymers of nBA and MMA to improve thermomechanical properties and further correlate with magneto-optical properties for use in photonic devices.

References

1) Pavlopoulos, N. G., Kang, K. S., Holmen, L. N., Lyons, N. P., Akhoundi, F., Carothers, K. J., Pyun, J. (2020). Polymer and magnetic nanoparticle composites with tunable magneto-optical activity: role of nanoparticle dispersion for high Verdet constant materials. J. Mater. Chem. C, 8(16), 5417–5425. https://doi.org/10.1039/D0TC00077A
2) Korth, B. D., Keng, P., Shim, I., Bowles, S. E., Tang, C., Kowalewski, T., Pyun, J. (2006). Polymer-Coated Ferromagnetic Colloids from Well-Defined Macromolecular Surfactants and Assembly into Nanoparticle Chains. Journal of the American Chemical Society, 128(20), 6562–6563. https://doi.org/10.1021/ja0609147
3) Keng, P. Y., Shim, I., Korth, B. D., Douglas, J. F., & Pyun, J. (2007). Synthesis and Self-Assembly of Polymer-Coated Ferromagnetic Nanoparticles. *ACS Nano*, *1*(4), 279–292. https://doi.org/10.1021/nn7001213
4) Bull, M. M., Chung, W. J., Anderson, S. R., Kim, S., Shim, I.-B., Paik, H., & Pyun, J. (2010). Synthesis of ferromagnetic polymer coated nanoparticles on multi-gram scale with tunable particle size. J. Mater. Chem., 20(29), 6023–6025. https://doi.org/10.1039/C0JM01042A
5) Carothers, K. J., Lyons N. P., Pavlopoulosa, N. G., Kochenderfer, T. M., Phan, A., Shim, I., Norwood, R. A., & Pyun, J. (2021). Polymer Coated Magnetic Nanoparticles as Ultra-High Verdet Constant Materials: Correlation of Nanoparticle Size with Magnetic & Magneto-Optical Properties. (In progress)
6) P. Wang, I. Jeon, Z. Lin, M. D. Peeks, S. Savagatrup, S. E. Kooi, T. Van Voorhis and T. M. Swager, J. Am. Chem. Soc., 2018, 140, 6501–6508.
7) C.-K. Lim, M. J. Cho, A. Singh, Q. Li, W. J. Kim, H. S. Jee, K. L. Fillman, S. H. Carpenter, M. L. Neidig, A. Baev, M. T. Swihart and P. N. Prasad, Nano Lett., 2016, 16, 5451–5455.
8) A. Lopez-Santiago, H. R. Grant, P. Gangopadhyay, R. Voorakaranam, R. A. Norwood and N. Peyghambarian, Opt. Mater. Express, 2012, 2, 978–986.
9) A. Lopez-Santiago, P. Gangopadhyay, J. Thomas, R. A. Norwood and N. Peyghambarian, Appl. Phys. Lett., 2009, 96, 143302–143304.
10) V. Demir, P. Gangopadhyay, R. A. Norwood and N. Peyghambarian, Appl. Opt., 2014, 10, 2087–2092.
11) A. Lopez-Santiago, P. Gangopadhyay, J. Thomas, R. A. Norwood and N. Peyghambarian, All-Optical Magnetometer based on Magnetite Core-Polymer Shell Nanocomposite Material, Frontiers in Optics 2009/Laser Science XXV/Fall 2009 OSA Optics & Photonics Technical Digest, OSA Technical Digest (CD) (Optical Society of America, 2009), paper AThB2.
12) A. Miles, Y. Gai, P. Gangopadhyay, X. Wang, R. A. Norwood and J. J. Watkins, Opt. Mater. Express, 2017, 7, 2126–2140.
13) Amirsolaimani, B.; Gangopadhyay, P.; Persoons, A. P.; Showghi, S. A.; LaComb, L. J.; Norwood, R. A.; Peyghambarian, N. High Sensitivity Magnetometer Using Nanocomposite Polymers with Large Magneto-Optic Response. Opt. Lett. 2018, 43, 4615.
14) Matyjaszewski, K.; Xia, J. Atom Transfer Radical Polymerization. *Chem. Rev.* 2001, *101*, 2921–2990.
15) R. Bahuguna, M. Mina, J.-W. Tioh and R. J. Weber, IEEE Trans. Magn., 2006, 42, 3099–3101.
16) Polymer properties database (n.d.). From http://polymerdatabase.com/polymer%20chemistry/pc%20index.html
17) Kampferback, M.; Vossmeyer, T.; Weller, H. (2019). Cross-Linked Polystyrene Shells Grown on Iron Oxide Nanoparticles via Surface-Grafted AGET-ATRP in Microemulsion. Langmuir, *35*, 8790-8798
18) Borozenko, O.; Machado, V.; Skene, W. G.; Giasson, S. Organophosphonic acids as viable linkers for the covalent attachment of polyelectrolyte brushes on silica and mica surfaces. (2014) Polym. Chem. 5, 5740.